CrossMark

TECHNICAL COMMUNICATION

# Sensitivity Analysis of the Main Factors Controlling Floor Failure Depth and a Risk Evaluation of Floor Water Inrush for an Inclined Coal Seam

**Weitao Liu[1] · Dianrui Mu[1] · Xiangxiang Xie[1] · Li Yang[2] · Donghui Wang[1]**

**Abstract** The main factors controlling floor failure depth are highly consistent with those of floor water inrush. In this paper, a mechanical model was developed to calculate the maximum failure depth of the upper and lower sides of a mining working face floor along the coal seam's inclination. The results indicated that the main factors controlling floor failure depth are mining thickness, working face slanting length, coal seam dip angle, mining depth, water pressure, cohesion, and internal friction angle. The floor failure depth of the 3303 working face in the Yangcheng coal mine was calculated using FLAC[3D] numerical simulation software. Based on matrix and variance analyses, the sensitivity of each of these factors with respect to floor failure depth followed the order: working face slanting length (extremely significant) > mining depth (highly significant) > cohesion (significant) > mining thickness (not significant) > coal seam dip angle (not significant) > water pressure (not significant) > internal friction angle (not significant). Also, the optimal plan for orthogonal simulation is $A_1 B_1 C_1 D_1 E_2 F_1 G_1$, in which the floor failure depth is minimized. Finally, the average accuracy of logistic regression analysis of the principal component was up to 90.4% accurate, about 10% better than conventional logistic regression analysis.

**Keywords** Floor aquiclude · Variance analysis · Principal component · Logistic regression analysis

✉ Dianrui Mu
  1731799913@qq.com

[1] College of Mining and Safety Engineering, Shandong University of Science and Technology, Qingdao 266590, China

[2] College of Foreign Languages, Shandong University of Science and Technology, Qingdao 266590, China

## Introduction

With increasing exploitation depths, safe production in China's coal mines will be severely constrained by floor water inrush accidents, which not only cause casualties and economic losses but also has enormous impacts to the area's water resources and environment (Peng and Wang 2001; Zhang et al. 1997). The mechanisms underlying floor strata deformation and failure depth have been studied (Cheng et al. 1999; Feng et al. 2009; Li and Gao 2003). Currently, there are many techniques for detecting the failure depth of a coal seam floor, including the mine electric profiling method, mine geological radars, the borehole wave velocity layer detection technique, the DC resistivity method, and CT technology (Wang 2000; Wang et al. 2010). The evaluation methods used for analyzing coal seam floor water inrush include support vector machines (Cao and Zhao 2011; Jiang and Liang 2005), the vulnerability index method (Wu et al. 2006, 2009), expert systems (Cao and Zhao 2011; Gao et al. 2009; Jiang and Liang 2005; Wu et al. 2006, 2009), and the water inrush coefficient method (Zhou et al. 2014). Of these, the water inrush coefficient method has been subject to considerable development because it is easy and quick to calculate.

In recent years, many experts and scholars have researched the failure depth of a coal seam floor and methods for evaluating floor water inrush. Using an orthogonal test design scheme, Liu et al. (2015) used FLAC[3D] to simulate floor failure depth and analyzed their results using variance analysis to study the sensitivity of the main factors controlling floor failure depth. Lu and Yao (2014) concluded that for a transversely isotropic floor, field measurements of the greatest failure depth and its location were generally consistent with those calculated based on the anisotropy of floor rock deformation and its strength. Li (1999) presented the

"lower three zones" methodology, which reflects the floor deformation and failure rule and the formation of a water inrush channel; this theoretical method has great guiding significance for the prevention and treatment of floor water inrush. Using previous water inrush data, Zhang et al. (2013) established a Fisher discriminant analysis model of floor water inrush risk and accurately predicted the inrush risk of test samples using the distance discriminant method.

Although these theoretical methods are useful for prediction of floor water inrush, there are still some issues. First, research on the failure depth of mine floors has focused mostly on horizontal and near-horizontal coal seams; the influence of the coal seam dip angle is seldom considered. Hence, the formula used to calculate floor failure depth is not suitable for an inclined coal seam. Second, in previous sensitivity analyses, the main factors controlling floor failure depth were mostly based on field experience, lacked any theoretical basis, and only analyzed sensitivity of the main factors without assessing how these may have affected each level differently. Finally, logistic regression analysis is only suitable for linearly independent variables, not for floor water inrush evaluation. Therefore, we used two methods of regression analysis to study the sensitivity of the main factors controlling floor failure depth. Logistic regression analysis of the principal components was conducted on the main factors controlling floor water inrush and an inrush evaluation model was established that not only addresses the limitations of linear dependent variables in logistic regression analysis but also improves the precision of logistic regression analysis in establishing a floor water inrush evaluation model.

## Methods

### Calculation of Mining Floor Failure Depth along the Direction of the Coal Seam

Under the influence of the working face abutment pressure, plastic failure of the working face floor rock occurs, forming a floor failure area. Based on floor slip line field theory, Zhang et al. (1997) presented the abutment pressure distribution of the floor along the direction of the coal seam (Fig. 1) and calculated the maximum failure depth as follows:

$$h_{\max} = \frac{L_a \cos \varphi_0}{2 \cos(\pi/4 + \varphi_0/2)} e^{(\pi/4 + \varphi_0/2) \tan \varphi_0} \tag{1}$$

where $H_m$ is the height of the caving zone, m; $\gamma H$ is the original rock stress in front of the coal wall, MPa; $k\gamma H$ is the working face advance support force, MPa; $\gamma H_m$ is the load above the caving zone in the goaf behind the coal wall, MPa;

I is the active limit region; II is the transition region; and III is the passive limit zone.

According to the limit equilibrium condition, the yield of the coal wall in front of the working face is

$$L_a = \frac{M}{2K_m \tan \varphi_m} \ln \frac{k\gamma H + C_m \cot \varphi_m}{K_m C_m \cot \varphi_m} \tag{2}$$

where $K_m = (1 + \sin\varphi_m)/(1 - \sin\varphi_m)$; $\varphi_m$ is the internal friction angle of the coal seam, °; $M$ is the thickness of the coal seam, m; $k$ is the working face advance support pressure concentration factor; $H$ is the burial depth of the coal seam, m; $\gamma$ is the average bulk density of the coal seam floor rock mass, kN·m$^{-3}$; and $\varphi_0$ is the average internal friction angle of the coal seam floor, °.

### Calculation of Floor Failure Depth along the Inclination Direction of the Coal Seam

To study the floor failure depth of the working face along the inclination direction, the coal seam floor in that direction can be simplified as a spatial semi-infinite body (Xu 2007), and the side-directed abutment pressure of the working face sides can be decomposed into a longitudinal load that is perpendicular to the coal seam and a transverse load that is parallel to the coal seam. This load can be simplified to an equivalent linear load, which is respectively loaded to a semi-infinite space. According to ground pressure theory and spatial semi-infinite body theory in elastic mechanics, combined with the side abutment pressure distribution characteristics for both sides of the working face in inclined coal seam longwall mining, a mechanical model of floor failure depth along the inclination direction of the coal seam (Fig. 2) and a mechanical calculation model of the floor under a distributed load (Fig. 3) were established.

According to the mechanical calculation model (Fig. 3), for a small unit of $d\varepsilon = \rho d\theta/\sin\theta$, where the ordinate origin o is $\varepsilon$, according to the spatial semi-infinite body theory in elastic mechanics, and the stress at the point of $M$ is caused by the transverse loads $dF$ acting on the small unit of $d\varepsilon$ at the boundary of semi-infinite space is:

$$\begin{cases} d\sigma_x = -\frac{2q}{\pi}\cos^2\theta d\theta \\ d\sigma_y = -\frac{2q}{\pi}\sin^2\theta d\theta \\ d\tau_{xy} = -\frac{2q}{\pi}\sin\theta\cos\theta d\theta \end{cases} \tag{3}$$

Integrating both sides of Eq. (3), the stress at the point of $M$ caused by all of the longitudinal distribution loads

(perpendicular to the direction of the coal body) acting on the mine floor is:

$$
\begin{cases}
\sigma_x = -\dfrac{2}{\pi} \displaystyle\int_{\theta_1}^{\theta_2} q\cos^2\theta \, d\theta \\[2mm]
\sigma_y = -\dfrac{2}{\pi} \displaystyle\int_{\theta_1}^{\theta_2} q\sin^2\theta \, d\theta \\[2mm]
\tau_{xy} = -\dfrac{2}{\pi} \displaystyle\int_{\theta_1}^{\theta_2} q \sin\theta \cos\theta \, d\theta
\end{cases}
\tag{4}
$$

Similarly, the stress at the point of $M$ caused by all of the transverse distribution loads (parallel to the direction of the coal body) acting on the floor is:

$$
\begin{cases}
\sigma_x = -\dfrac{2}{\pi} \displaystyle\int_{\theta_1}^{\theta_2} q'\dfrac{\cos^3\theta}{\sin\theta} \, d\theta \\[2mm]
\sigma_y = -\dfrac{2}{\pi} \displaystyle\int_{\theta_1}^{\theta_2} q' \sin\theta \cos\theta \, d\theta . \\[2mm]
\tau_{xy} = -\dfrac{2}{\pi} \displaystyle\int_{\theta_1}^{\theta_2} q'\cos^2\theta \, d\theta
\end{cases}
\tag{5}
$$

The intensities of the distribution loads for the coal seam along the inclination direction are expressed as:

$$
\begin{cases}
q_1 = \dfrac{k_1 + 1}{2}\gamma H_1 \cos\alpha \\[2mm]
q_2 = \dfrac{k_2 + 1}{2}\gamma H_2 \cos\alpha \\[2mm]
q_3 = \left(P_1 - \dfrac{l_1 \Delta P}{2L}\right)\cos\alpha \\[2mm]
q_4 = \left(P_2 + \dfrac{l_2 \Delta P}{2L}\right)\cos\alpha
\end{cases}
\tag{6}
$$

$$
\begin{cases}
q_5 = \dfrac{k_1 + 1}{2}\gamma H_1 \sin\alpha \\[2mm]
q_6 = \dfrac{k_2 + 1}{2}\gamma H_2 \sin\alpha \\[2mm]
q_7 = \left(P_1 - \dfrac{l_1 \Delta P}{2L}\right)\sin\alpha \\[2mm]
q_8 = \left(P_2 + \dfrac{l_2 \Delta P}{2L}\right)\sin\alpha
\end{cases}
\tag{7}
$$

$$
\begin{cases}
H_1 = H - \dfrac{l_1 \sin\alpha}{2} \\[2mm]
H_2 = H' + \dfrac{l_2 \sin\alpha}{2}
\end{cases}
\tag{8}
$$

where $q_1$, $q_2$, $q_3$, $q_4$ are longitudinal load intensities on the floor of the coal seam, kN·m$^{-1}$; $q_6, q_7, q_8, q_9$ are transverse load intensities on the floor of the coal seam, kN·m$^{-1}$; $\alpha$ is the dip angle of the coal seam, °; $P_1$ is the water pressure of the upper crossheading of the working face, MPa; $P_2$ is the water pressure of the lower crossheading of the working face, MPa; $\Delta P$ is the water pressure difference between the upper and lower crossheading of the working face; $H$ and $H'$ are the buried depth of the upper and lower crossheading of the working face, respectively, m; $H_1$ and $H_2$ are the buried depth of the lateral abutment pressure peak on the upper and lower sides of the working face, respectively, m; $\gamma$ is the average bulk density of the rock mass in the stope floor, kN·m$^{-3}$; $l_1$ and $l_2$ are the slanting length of the stress concentration zone of the coal floor in the upper and lower sides of the working face, respectively, m; and $k_1$ and $k_2$ are the lateral support pressure concentration factor of both sides of the working face, respectively, where $k_2 > k_1$. Substituting Eqs. (6) and (7) into Eqs. (4) and (5), respectively, the horizontal stress and shear stress at any point in the floor along the inclination direction can be obtained as follows:

Fig. 1 The abutment pressure distribution of a mining floor along the direction of the coal seam
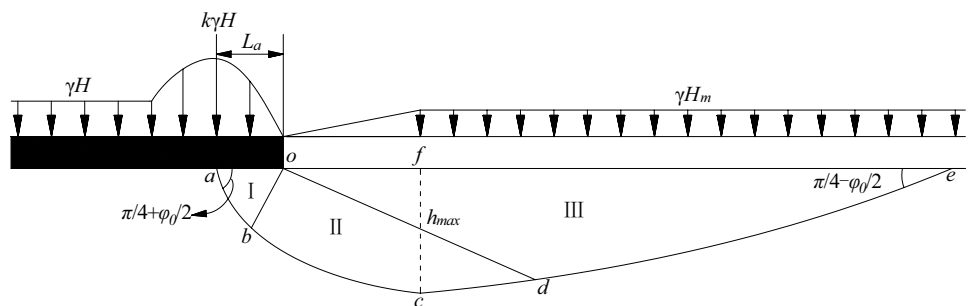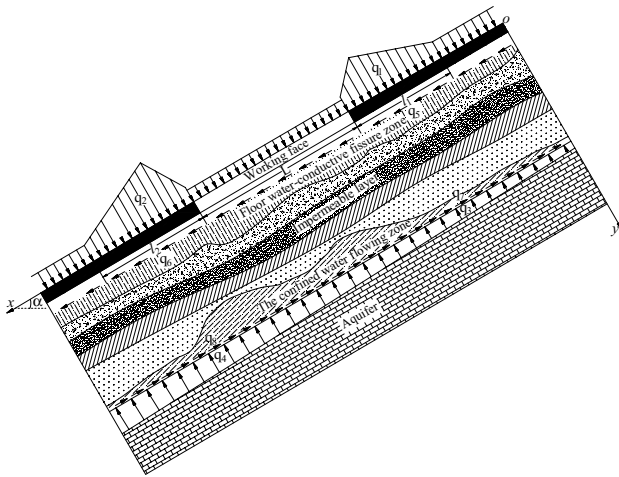
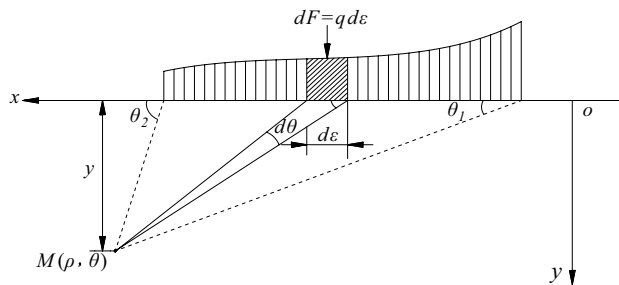**Fig. 2** Mechanical calculation model of floor failure depth along the inclination direction of the coal seam



**Fig. 3** Mechanical calculation model of a mining floor under a distributed load

$$
\begin{cases}
\sigma_x = -\dfrac{2}{\pi}\left(\displaystyle\int_{\theta_1}^{\theta_2} q\cos^2\theta\, d\theta + \int_{\theta_1}^{\theta_2} q'\dfrac{\cos^3\theta}{\sin\theta}\, d\theta\right)\\[4pt]
\quad = \dfrac{q}{\pi}\left[\theta_1 - \theta_2 + \sin(\theta_1 - \theta_2)\cos(\theta_1 + \theta_2)\right] +\\[4pt]
\quad\quad \dfrac{q'}{\pi}\left[2\ln\dfrac{\sin\theta_1}{\sin\theta_2} - \sin(\theta_1 - \theta_2)\sin(\theta_1 + \theta_2)\right]\\[4pt]
\sigma_y = -\dfrac{2}{\pi}\left(\displaystyle\int_{\theta_1}^{\theta_2} q\sin^2\theta\, d\theta + \int_{\theta_1}^{\theta_2} q'\sin\theta\cos\theta\, d\theta\right)\\[4pt]
\quad = \dfrac{q}{\pi}\left[\theta_1 - \theta_2 - \sin(\theta_1 - \theta_2)\cos(\theta_1 + \theta_2)\right] +\\[4pt]
\quad\quad \dfrac{q'}{\pi}\left[\sin(\theta_1 - \theta_2)\sin(\theta_1 + \theta_2)\right]\\[4pt]
\tau_{xy} = -\dfrac{2}{\pi}\left(\displaystyle\int_{\theta_1}^{\theta_2} q\sin\theta\cos\theta\, d\theta + \int_{\theta_1}^{\theta_2} q'\cos^2\theta\, d\theta\right)\\[4pt]
\quad = \dfrac{q}{\pi}\left[\sin(\theta_1 - \theta_2)\sin(\theta_1 + \theta_2)\right] +\\[4pt]
\quad\quad \dfrac{q'}{\pi}\left[\theta_1 - \theta_2 + \sin(\theta_1 - \theta_2)\cos(\theta_1 + \theta_2)\right]
\end{cases}
\tag{9}
$$

According to the theory of elastic mechanics, the principal stress at any point in the coal seam floor is:

$$
\sigma_1, \sigma_3 = \frac{\sigma_x - \sigma_y}{2} \pm \sqrt{\left(\frac{\sigma_x - \sigma_y}{2}\right)^2 + \tau_{xy}^2}.
\tag{10}
$$

Based on equations (9) and (10), and considering the effects of the coal floor weight, the principal stress at any point in the working face floor is:

$$
\begin{cases}
\sigma_1 = \dfrac{q(\theta_1 - \theta_2)}{\pi} + \dfrac{1}{\pi}\left[\sqrt{q^2 + q'^2}\,\sin(\theta_1 - \theta_2) + q'(\theta_1 - \theta_2)\right] - \dfrac{\gamma y}{\cos\alpha}\\[6pt]
\sigma_3 = \dfrac{q(\theta_1 - \theta_2)}{\pi} - \dfrac{1}{\pi}\left[\sqrt{q^2 + q'^2}\,\sin(\theta_1 - \theta_2) + q'(\theta_1 - \theta_2)\right] - \dfrac{\gamma y}{\cos\alpha}
\end{cases}
\tag{11}
$$

The uniform load on the upper side of the working face mining floor is:

$$
\begin{cases}
q = \left[\dfrac{(k_1 + 1)\gamma H_1}{2} - \left(P_1 - \dfrac{l_1\Delta P}{2L}\right)\right]\sin\alpha\\[6pt]
q' = \left[\dfrac{(k_1 + 1)\gamma H_1}{2} - \left(P_1 - \dfrac{l_1\Delta P}{2L}\right)\right]\cos\alpha
\end{cases}.
\tag{12}
$$

Substituting Eq. (12) into Eq. (11), the principal stress at any point on the upper side of the working face mining floor is:

$$
\begin{cases}
\sigma_1 = \dfrac{1}{\pi}\left[\dfrac{(k_1 + 1)\gamma H_1}{2} - \left(P_1 - \dfrac{l_1\Delta P}{2L}\right)\right]\\[6pt]
\quad [\theta(\sin\alpha + \cos\alpha) + \sin\theta] - \gamma\left[\dfrac{y}{\cos\alpha} + \dfrac{M}{(\lambda - 1)\cos\alpha}\right]\\[6pt]
\sigma_3 = \dfrac{1}{\pi}\left[\dfrac{(k_1 + 1)\gamma H_1}{2} - \left(P_1 - \dfrac{l_1\Delta P}{2L}\right)\right]\\[6pt]
\quad [\theta(\cos\alpha - \sin\alpha) - \sin\theta] - \gamma\left[\dfrac{y}{\cos\alpha} + \dfrac{M}{(\lambda - 1)\cos\alpha}\right]
\end{cases},
\tag{13}
$$

where $\theta = \theta_1 - \theta_2$; $y$ is the plastic failure depth of the upper side of the working face mining floor; and the other parameters are the same as those above.

When plastic deformation occurs at any point of the working face floor, the principal stress is satisfied by the limit equilibrium condition. According to the Mohr–Coulomb yield criterion in geotechnical engineering, the following equation can be obtained:

$$
\frac{1}{2}(\sigma_1 - \sigma_3) = C\cos\varphi_0 + \frac{1}{2}(\sigma_1 + \sigma_3)\sin\varphi_0,
\tag{14}
$$

where $C$ is the average cohesive force of the rock mass in the coal seam floor, MPa; $\varphi_0$ is the average internal friction angle of the rock mass in the coal seam floor, °; $\sigma_1$ and $\sigma_3$ are the maximum and minimum principal stress of the rock mass in the coal seam floor, respectively, MPa. Based on equations (13) and (14), the failure depth of the upper side of the working face floor is:

$$y = \frac{\cos\alpha}{\pi\gamma}\left[\frac{(k_1+1)\gamma H_1}{2} - \left(P_1 - \frac{l_1\Delta P}{2L}\right)\right]$$
$$\left[\theta\left(\cos\alpha - \frac{\sin\alpha}{\sin\varphi_0}\right) - \frac{\sin\theta}{\sin\varphi_0}\right] + \frac{C\cos\alpha}{\gamma\tan\varphi_0} + \frac{M}{(\lambda-1)}. \tag{15}$$

We set $dy/d\theta = 0$: $\beta = \arccos(\cos\alpha \sin\varphi_0 - \sin\alpha)$. By setting $\beta = \arccos(\cos\alpha \sin\varphi_0 - \sin\alpha)$, and substituting $\beta$ into Eq. (15), the maximum failure depth of the upper side of the working face floor is:

$$h_{up} = \frac{\cos\alpha}{\pi\gamma}\left[\frac{(k_1+1)\gamma H_1}{2} - \left(P_1 - \frac{l_1\Delta P}{2L}\right)\right]$$
$$\left[\theta\left(\cos\alpha - \frac{\sin\alpha}{\sin\varphi_0}\right) - \frac{\sin\theta}{\sin\varphi_0}\right] + \frac{C\cos\alpha}{\gamma\tan\varphi_0} + \frac{M}{(\lambda-1)}. \tag{16}$$

Similarly, the maximum failure depth of the lower side of the working face floor is:

$$h_{down} = \frac{\cos\alpha}{\pi\gamma}\left[\frac{(k_2+1)\gamma H_2}{2} - \left(P_2 + \frac{l_2\Delta P}{2L}\right)\right]$$
$$\left[\theta\left(\cos\alpha - \frac{\sin\alpha}{\sin\varphi_0}\right) - \frac{\sin\theta}{\sin\varphi_0}\right] + \frac{C\cos\alpha}{\gamma\tan\varphi_0} + \frac{M}{(\lambda-1)}. \tag{17}$$

where $\beta = \arccos(\cos\alpha \sin\varphi_0 - \sin\alpha)$; and the other parameters are the same as those above. Based on equations (1), (16), and (17), the expression for the coal seam floor failure depth contains 11 parameters: $M$, $k$, $H$, $P$, $L$, $C$, $\varphi_m$, $\lambda$, $C_m$, $\alpha$, and $\varphi_0$, where the parameters $M$, $L$, $\alpha$, $H$, $P$, $C$, and $\varphi_0$ are the main control parameters. Considering field engineering practice and measured mining floor failure depths, we selected seven factors (mining thickness, working face slanting length, coal seam dip angle, mining depth, water pressure, cohesion, and internal friction angle) as the main control factors in a numerical simulation test.

## Analysis of the Main Control Factors of Mining Floor Failure Depth

In essence, floor water inrush is the process of floor-confined water breaking through the aquifuge into the goaf under the influence of many factors. According to the "lower three zone" theory, the relative aquifuge between a coal seam and an underlying aquifer is divided into the mine pressure failure zone, the effective protective zone, and the confined water guide zone. When the confined water guide zone is connected to the mine pressure failure zone, floor water inrush occurs.

According to engineering practice, the general trends regarding the influence of the main control factors of floor failure depth have the following characteristics: (1) Greater mining thickness results in a more mine pressure, which increases suddenly, and a greater failure degree of the coal seam floor. (2) A longer working face slanting length results in a greater floor failure depth. (3) The failure depth of the coal seam floor initially increases, followed by a decrease as the coal seam dip angle increases, because the change in the coal seam angle influences the stress concentration effect of the rock mass, which complicates the change in the seam floor failure depth. (4) Greater mining depth results in greater stress and water pressure and more serious floor failure. (5) When the water pressure is higher, the failure depth of the upper side of the working face floor is larger, and the floor failure depth of the lower side of the working face floor is smaller; the coal floor failure depth is also greatly influenced by the combined effect of other factors. (6) A greater cohesion and internal friction angle results in a greater anti-shear capacity of the coal seam floor and a smaller failure depth of the coal seam floor.

Most of North China's inclined coal seams have a dip angle of 25°–35°, and coal seam floor lithology is different in different mine areas (cohesion, internal friction angle), so methods of coal seam mining (mining thickness, working face slanting length, mining depth, etc.) must also differ. To reflect the process and characteristics of floor rock failure, considering the practical production of China's coal and the general characteristics of mining conditions, we determined the level values of the main control factors of floor failure depth (Table 1).

## Orthogonal Simulation Calculation of Mining Floor Failure Depth

### Engineering Background and Selection of Simulation Range

The 3308 working face of the Yangcheng coal mine is a longwall arrangement; coal 3 is the main seam, with a ground elevation of +37.3 to +38.2 m and a working face elevation of −800 to −940 m. The coal seam is 6.7 m thick, the seam dip angle is 27°–33°, with an average angle of 30°, the length of the working face is 452 m, and the slanting length is 150 m. Floor limestone water is the greatest threat to the working face; its hydrostatic pressure is 1.98 MPa.

Based on the geological mining conditions of this working face, Mohr–Coulomb mechanical constitutive models were used to create a numerical model (Fig. 4). In the model, the inclination ($x$) is 200 m, the strike ($y$) is 220 m, and the height ($z$) is 285 m, yielding a total of 159,250 units and

169,848 nodes. The longwall working face proceeds in steps, with a 35 m retaining protective pillar on each side of the working face. Each step excavates 10 m along the seam, for 15 steps, which moves the working face 150 m forward. The mechanical conditions of the model are: the x and y direction of the front, rear, left, and right boundaries are fixed, the bottom is a fully-constrained boundary, the top boundary of the model is equivalent to the weight of the upper rock mass at a certain load, and calculations show that the top loading surface pressure is 7.2 MPa. Meanwhile, for the flow: the bottom of the fixed water pressure boundary was used to simulate the confined water value (1.98 MPa) of the 3rd limestone aquifer, and the initial water pressure of the bottom plate was changed according to the gradient water pressure; the other boundary is a water-resisting boundary. After the working face was mined, the goaf was taken as a drainage boundary, without considering the water in the goaf, the border of which was fixed with zero pressure.

*Simulation Test Scheme and Results Analysis*

To study the sensitivity of the previously listed factors determining the floor failure depth, an orthogonal test design method was adopted, considering various levels of the main controlling factors and the processing and calculation complexity (Chen 2005). The program can effectively reduce the computational work by using an orthogonal table to determine the numerical simulation test. The orthogonal design method was used to design a mixed orthogonal test table L18 ($2 \times 3^7$), namely, the first factors for 2 levels, followed by 7 factors for 3 levels. According to this design scheme, the floor failure depth of the 3303 working face was simulated and tested, allowing the floor failure depths to be obtained under different test schemes (Table 2).

As shown in Table 2, the floor failure depths of the 3, 5, 6, 8, 9, 12, 13, 15, 17, 18 test schemes were higher than the average floor failure depth (14 m), with the failure depth of test 3 being the largest (20 m). In the 1, 2, 4, 10, 11, 14, 16 test schemes, the floor failure depths were less than 14 m, with the floor failure depth of test 1 being the smallest (8 m). According to the numerical simulation, test 1 was initially confirmed as the optimal orthogonal test scheme in the 18 groups.

# Results and Discussion

## Sensitivity Analysis of the Main Control Factors of Floor Failure Depth

### Matrix Analysis of the Orthogonal Test Design

The floor failure depths were calculated under different test schemes according to the simulation results and the ranges of the main controlling factors were determined (Table 3). This range analysis was used to determine the sensitivity of each main controlling factor.

The mean change in the main control factors at different levels of floor failure depth show that as the working face slanting length and mining depth increase, floor failure depth increases at a growing rate. For increased cohesion, the floor failure depth was gradually reduced, causing the rate of decrease to become increasingly smaller. For an increased mining thickness, the floor failure depth gradually increases, with the rate of growth becoming increasingly smaller. As the coal seam dip angle increases, the floor failure depth initially increases and then decreases; the floor failure depth reaches a maximum when the coal seam dip angle is approximately 30°, which is consistent with previous findings that the rock mass of the floor is more prone to slip shear failure when the coal seam dip angle is approximately 30°–35° (Sun 2014). For increased water pressure and internal friction angle, the floor failure depth generally decreases.

The range analysis results for the main controlling factors was: $R_B$ (5.8) > $R_D$ (3.0) > $R_F$ (2.6) > $R_A$ (1.3) > $R_C$ (1.0) > $R_E$ (0.9) > $R_G$ (0.7), i.e., the order of sensitivity of the main control factors of floor failure depth was working face slanting length > mining depth > cohesive force > mining thickness > seam dip > pressure > internal friction angle. The range values of the working face slanting length, mining depth, and cohesion exceeded the range average (2.2). Obviously, these same three factors dominated, with the maximum sensitivity displayed by the working face slanting length, with range values up to 5.8. Of mining depth and cohesion, the range of the former was slightly larger. The sensitivities of mining thickness, coal seam dip angle, water pressure, and internal friction angle were low, with a range that was obviously less than the average (Fig. 5).

The weight matrix of the main control factors of floor failure depth is denoted as *K*; the magnitude of the elements in the matrix reflects the strength of the influence of the main control factors of floor failure depth:

**Table 1** The level values of the main control factors of floor failure depth

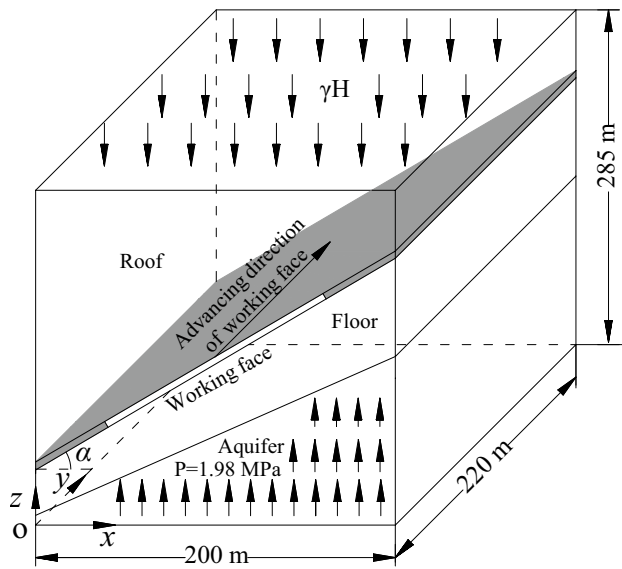| Main control factors | Level 1 | Level 2 | Level 3 |
|---|---|---|---|
| Mining thickness A | 3 | 5 | 6.7 |
| Working face slanting length B | 50 | 100 | 150 |
| Coal seam dip angle C | 25 | 30 | 35 |
| Mining depth D | 500 | 700 | 900 |
| Water pressure E | 1 | 2 | 3 |
| Cohesion F | 6 | 4 | 2 |
| Internal friction angle G | 40 | 30 | 20 |

**Fig. 4** Numerical calculation model of an inclined seam in a longwall mining excavation

$$K = \begin{bmatrix} 1/K_{11} & 0 & 0 & \ldots & 0 \\ \ldots & \ldots & \ldots & \ldots & \ldots \\ 1/K_{1n} & 0 & 0 & \ldots & 0 \\ 0 & 1/K_{21} & 0 & \ldots & 0 \\ \ldots & \ldots & \ldots & \ldots & \ldots \\ 0 & 1/K_{2n} & 0 & \ldots & 0 \\ \ldots & \ldots & \ldots & \ldots & \ldots \\ 0 & 0 & 0 & \ldots & 1/K_{m1} \\ \ldots & \ldots & \ldots & \ldots & \ldots \\ 0 & 0 & 0 & \ldots & 1/K_{mn} \end{bmatrix} \begin{bmatrix} T_1 & 0 & \ldots & 0 \\ 0 & T_2 & \ldots & 0 \\ \ldots & \ldots & \ldots & \ldots \\ 0 & 0 & \ldots & T_m \end{bmatrix} \begin{bmatrix} S_1 \\ S_2 \\ \ldots \\ S_m \end{bmatrix}$$

$$(18)$$

where $m$ is the factor number and $n$ is the level number in the orthogonal test (in this scheme, $m = 7$, $n = 3$). The smaller the floor failure depth, the better. The elements of the experimental investigation index layer matrix are $k_{ij} = 1/Kij$, $i = 1$, $2 \ldots 6$, 7, $j = 1$, 2, 3; the elements of the factor layer matrix are $T_i = 1 / \sum_{j=1}^{n} 1/K_{ij}$, $i = 1$, $2 \ldots 6$, 7; the elements of the horizontal layer matrix $S_i = R_i / \sum_{i=1}^{m} R_i$, $i = 1$, $2 \ldots 6$, 7; and the other parameters are the same as those above.

By substituting the data from the range analysis table of the main control factors of floor failure depth into Eq. (18),

**Table 2** The orthogonal simulate test scheme of floor failure depth and results

| Test scheme | Main control factors | | | | | | | | Floor failure depth (m) |
|---|---|---|---|---|---|---|---|---|---|
| | Empty column | Mining thickness A (m) | Working face slanting length B (m) | Coal seam dip angle C (°) | Mining depth D (m) | Water pressure E (MPa) | Cohesion F (MPa) | Internal friction angle G (°) | |
| 1 | 1 | 1(3) | 1 (50) | 1 (25) | 1 (500) | 1 (1) | 1 (6) | 1 (40) | 8 |
| 2 | 1 | 1 | 2 (100) | 2 (30) | 2 (700) | 2 (2) | 2 (4) | 2 (30) | 12 |
| 3 | 1 | 1 | 3 (150) | 3 (35) | 3 (900) | 3 (3) | 3 (2) | 3 (20) | 20 |
| 4 | 1 | 2 (5) | 1 | 1 | 2 | 2 | 3 | 3 | 12 |
| 5 | 1 | 2 | 2 | 2 | 3 | 3 | 1 | 1 | 14 |
| 6 | 1 | 2 | 3 | 3 | 1 | 1 | 2 | 2 | 15 |
| 7 | 1 | 3 (6.7) | 1 | 2 | 1 | 3 | 2 | 3 | 10 |
| 8 | 1 | 3 | 2 | 3 | 2 | 1 | 3 | 1 | 16 |
| 9 | 1 | 3 | 3 | 1 | 3 | 2 | 1 | 2 | 16 |
| 10 | 2 | 1 | 1 | 3 | 3 | 2 | 2 | 1 | 11 |
| 11 | 2 | 1 | 2 | 1 | 1 | 3 | 3 | 2 | 11 |
| 12 | 2 | 1 | 3 | 2 | 2 | 1 | 1 | 3 | 16 |
| 13 | 2 | 2 | 1 | 2 | 3 | 1 | 3 | 2 | 15 |
| 14 | 2 | 2 | 2 | 3 | 1 | 2 | 1 | 3 | 11 |
| 15 | 2 | 2 | 3 | 1 | 2 | 3 | 2 | 1 | 17 |
| 16 | 2 | 3 | 1 | 3 | 2 | 3 | 1 | 2 | 11 |
| 17 | 2 | 3 | 2 | 1 | 3 | 1 | 2 | 3 | 15 |
| 18 | 2 | 3 | 3 | 2 | 1 | 2 | 3 | 1 | 18 |

the weight matrix of floor failure depth can be obtained as follows:

$$
\begin{aligned}
k &= [A_1, A_2, A_3, B_1, B_2, B_3, C_1, C_2, C_3, D_1, D_2, D_3, E_1, E_2, E_3, F_1, F_2, F_3, G_1, G_2, G_3]^T \\
&= [0.030, 0.028, 0.027, 0.151, 0.128, 0.100, 0.023, 0.021, 0.021, 0.073, 0.064, \\
&\quad 0.059, 0.019, 0.020, 0.019, 0.061, 0.058, 0.051, 0.016, 0.015, 0.015]^T
\end{aligned}
$$

The weight calculation results show that $A_1$ is the maximum weight for factor A (0.030), $B_1$ for factor B (0.151), $C_1$ for factor C (0.023), $D_1$ for factor D (0.073), $E_2$ for factor E (0.020), $F_1$ for factor F (0.061), and $G_1$ for factor G (0.016). The different weights of the main control factors reflect the different impacts on the floor failure depth at different levels; a greater value indicates a less destructive effect on the floor at this level. Therefore, the optimal scheme of the orthogonal simulation test can be determined as $A_1 B_1 C_1 D_1 E_2 F_1 G_1$, which can effectively reduce the risk of floor water inrush with the smallest floor failure depth. The average weight of the different levels of each main control factor is, respectively: factor A (0.028), factor B (0.126), factor C (0.022), factor D (0.065), factor E (0.019), factor F (0.057), and factor G (0.015). Therefore, the sensitivity order of the main control factors of floor failure depth is B > D > F > A > C > E > G, namely, working face slanting length > mining depth > cohesion > mining thickness > coal seam dip angle > hydraulic > internal friction angle, which is consistent with the results obtained using the range analysis method.

### Variance Analysis of the Orthogonal Test Design

In orthogonal experimentation, the experimental index value results (floor failure depth) of the simulation test are analyzed and processed, and a variance analysis of the orthogonal experiment design is performed (Table 4). The data in the variance analysis table show the following results: the derivate square of the test error is relatively small (2.07), so the test error can be ignored. This means that the variance analysis of the main control factors of floor failure depth is better. Based on the significance test (F value) of the main controlling factors, the working face slanting length is highly significant (> 18), the mining depth and cohesion are significant, and the mining depth is slightly more significant than cohesion (> 6.94 and < 18). The other factors are not significant (< 6.94). The order of influence is: working face slanting length (50.94) > mining depth (13.26) > cohesion (11.16) > mining thickness (2.79) > coal seam dip angle (1.66) > water pressure (1.01) > internal friction angle (0.86), which is consistent with the results obtained using the matrix analytical method.

In the process of coal mining, the abutment pressure of the first cut on the working face and the floor in front of the coal wall is concentrated, and the stress of the floor rock mass in the gob is fully released, with a state of high pressure relief. Under these conditions, the gob floor is prone to upward bending deformation, threatening to induce water inrush through the floor. The mining and the floor heaving process aggravate the development, expansion, and penetration of fractures, leading to a constantly increasing guide height of floor-confined water. However, the mine floor failure depth gradually increases with the advance of the working face, which shortens the distance between the floor water-conducting failure zone and the floor confined water guide zone. The floor failure depth is a primary determinant of water inrush; therefore, a sensitivity analysis of the main factors controlling floor failure depth is critical in evaluating the likelihood of an inrush through the floor.

**Table 3** The range analysis table of the main control factors of floor failure depth

| Parameters | Main control factors | | | | | | |
|---|---|---|---|---|---|---|---|
| | Mining thickness A (m) | Working face slanting length B (m) | Coal seam dip angle C (°) | Mining depth D (m) | Water pressure E (MPa) | Cohesion F (MPa) | Internal friction angle G (°) |
| $k_1$ | 13.0 | 11.2 | 13.2 | 12.2 | 14.2 | 12.7 | 14.0 |
| $k_2$ | 14.0 | 13.2 | 14.2 | 14.0 | 13.3 | 13.3 | 13.3 |
| $k_3$ | 14.3 | 17.0 | 14.0 | 15.2 | 13.8 | 15.3 | 14.0 |
| R | 1.3 | 5.8 | 1.0 | 3.0 | 0.9 | 2.6 | 0.7 |
| $R_{avg}$ | | | | 2.2 | | | |

$k_1$, $k_2$ and $k_3$ are the average values of floor failure depth at the first, second and third levels of the main control factors, respectively; $R$ is the range value of each level of experimental factors, $R = \max\{k_1, k_2, k_3\} - \min\{k_1, k_2, k_3\}$, and a greater $R$ results in a greater impact on the floor failure depth of the main control factor at different levels and a stronger sensitivity; $R_{avg}$ is the range average of the main control factors

**Fig. 5** Range value histogram of main control factors
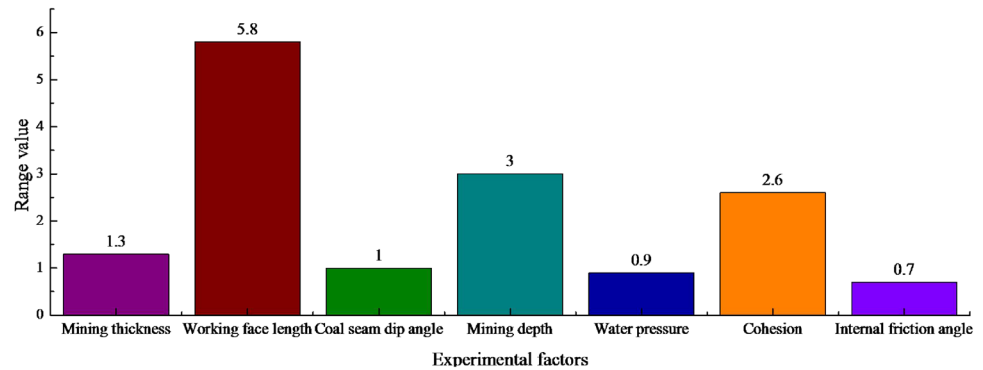


## Water Inrush Evaluation Model

Water inrush from mining floors is a complex geological phenomenon that is influenced by many factors, including lithology, hydrology, geology, and mining conditions. The water pressure indicates the dynamic condition of the floor water inrush, which is a strong determinant of its severity. To some degree, the cohesion and internal friction angle suppress floor water inrush, and their values are closely related to the floor failure depth. Mining depth, mining thickness, and working face slanting length indicate the mining disturbance conditions; the stability of a water-resisting floor primarily depends on these three values. The angle of the coal seam determines the spatial relationship of the mining field and the aquifer and influence the stress-disturbing effects. Thus, floor water inrush is primarily determined by a complex coupling relationship among various factors (Shi et al. 2015).

Experts and scholars have conducted research in different fields using established regression models. Rezaei et al. (2016) compared different mass transfer-based models with the Food and Agriculture Organization Penman–Monteith model to estimate potential evapotranspiration. Their results showed that the Albrecht model estimated potential evapotranspiration better than the other models. Valipour (2016) forecasted monthly rainfall using time series models and determined appropriate observation data for different climatic conditions. This showed that the accuracy of time series models increased with the amount of arid and humid climate observation data, and that these models were appropriate tools for forecasting monthly rainfall forecasting in semi-arid climates. Valipour et al. (2013) compared ARMA and ARIMA models with static and dynamic autoregressive artificial neural network models and showed that the ARIMA model had less error than the ARMA model in forecasting the inflow of a dam reservoir. To estimate potential evapotranspiration, five temperature-based, five radiation-based, and five mass transfer-based models were

selected with respect to performance in different climates based on earlier investigations. The Blaney–Criddle and Abtew models, respectively, were the best for estimating potential evapotranspiration in arid and semi-arid regions (Valipour et al. 2017).

### Logistic Regression Analysis of the Principal Components

SPSS software was used to integrate principal component analysis and logistic regression analysis, based on dimensionless treatment and superposition on each selected influence factor, to obtain the appropriate influence factor weighting. Based on dimension reduction of the principal component, this method transforms multiple highly correlated initial influence factors into a few low-correlation comprehensive influence factors (principal components) and then uses the principal component from the dimension reduction instead of the initial influence factors. The principal component analysis results are shown in Table 5.

The characteristic value of the principal component must be more than 1. Table 5 shows that the characteristic roots of the former 3 principal components: 2.014, 1.764, and 1.337, respectively; the cumulative contribution variance rate was 73.075%. Therefore, these 3 principal components met the evaluation requirements. According to Table 5, the main influence factors of the first principal component are the cohesion, length, and internal friction angle, respectively, with score coefficients of 0.400, 0.375, and 0.332, respectively. Because the proportion of cohesion and internal friction angle is larger, the floor lithology can be named as a principal component; the main influence factors of the second principal component are water pressure and coal seam dip angle, with score coefficients of 0.514 and 0.6868, respectively. Then the second principal component can be named as the main component of the hydrogeological conditions. The main influence factors of the third principal component are mining thickness and depth, with score coefficients of 0.584 and 0.489, respectively, and it can be

**Table 4** The variance analysis table of the main control factors of floor failure depth

| Parameters | Main control factors | | | | | | | Errors ($e^{\Delta}$) |
|---|---|---|---|---|---|---|---|---|
| | Mining thickness A (m) | Working face slanting length B (m) | Coal seam dip angle C (°) | Mining depth D (m) | Water pressure E (MPa) | Cohesion F (MPa) | Internal friction angle G (°) | |
| $S$ | 5.77 | 105.43 | 3.43 | 27.43 | 2.10 | 23.10 | 1.77 | 3.87 |
| $n$ | 2 | 2 | 2 | 2 | 2 | 2 | 2 | 4 |
| $S_{avg}$ | 2.89 | 52.72 | 1.72 | 13.72 | 1.05 | 11.55 | 0.89 | 0.97 |
| $F$ | 2.79 | 50.94 (**) | 1.66 | 13.26 (*) | 1.01 | 11.16 (*) | 0.86 | |

① $S$, $n$ and $S_{avg}$ are the deviations squares sum, degree of freedom and mean square sum of deviation, respectively. The ratio of the mean square sum of the deviation of the main control factors and that of the error is recorded as value $F$, which reflects the strength of the influence of the main control factors of floor failure depth; ② $F_{0.01}(2, 4) = 18$, $F_{0.05}(2, 4) = 6.94$, $F_{0.10}(2, 4) = 4.32$. when $F > F_{0.01}(2,4)$, the factor is highly significant, represented by * *; when $F_{0.05}(2,4) < F < F_{0.01}(2,4)$, the factor is significant, represented by *; when $F < F_{0.10}(2,4)$, the factor is not significant; ③ when $S < 2S_e$, the sum of squares of deviations of factors or interaction and degrees of freedom are incorporated into the error deviation square and degrees of freedom, recorded as $e^{\Delta}$, which improves the sensitivity of test $F$.

considered the main component of the geological mining conditions. Using principal component analysis theory and the principal component score coefficient, a linear relationship was established between the principal components and the main control factors:

$$\begin{cases} Y_1 = -0.111X_1 - 0.375X_2 + 0.139X_3 - 0.217X_4 + 0.085X_5 + 0.4X_6 + 0.332X_7 \\ Y_2 = 0.158X_1 + 0.088X_2 + 0.368X_3 - 0.290X_4 + 0.514X_5 - 0.101X_6 - 0.201X_7 \\ Y_3 = 0.584X_1 - 0.010X_2 - 0.322X_3 + 0.489X_4 - 0.023X_5 + 0.131X_6 + 0.216X_7 \end{cases} \quad (19)$$

where $X_1$ is the coal seam thickness, m; $X_2$ is the working face slanting length, m; $X_3$ is the seam dip angle, °; $X_4$ is the coal mining depth, m; $X_5$ is the confined water pressure, MPa; $X_6$ is the average cohesion of the rock bottom, MPa; $X_7$ is the average friction angle of the rock bottom, °; $Y_1$ is the floor lithologic main component; $Y_2$ is the main component of the hydrogeological conditions; and $Y_3$ is the main component of the geological mining conditions. By substituting the initial influence factors into the linear expression of $Y_1$, $Y_2$ and $Y_3$, comprehensive scores of the initial influence factors are obtained, which are used as the influence factors in regression analysis, followed by logistic regression analysis using SPSS software (Table 6). Moreover, the regression coefficients of $Y_1$, $Y_2$ and $Y_3$ are calculated to be 0.183, 0.638, and 0.438, and the regression constant is 1.216. Then a prediction model of floor water inrush can be established.

$$\begin{aligned} LogitP &= 0.183Y_1 + 0.638Y_2 + 0.438Y_3 + 1.216 \\ &= 0.336X_1 - 0.017X_2 + 0.401X_3 - 0.011X_4 \\ &\quad + 0.333X_5 + 0.066X_6 + 0.027X_7 + 1.216 \end{aligned} \quad (20)$$

By substituting each influence factor of floor water inrush into Eq. (20), the water inrush criteria can be obtained:

$$\begin{cases} \text{when } P > 0.5, \text{ floor water inrush may occur} \\ \text{when } P < 0.5, \text{ floor water inrush does not occur} \end{cases}$$

Goodness-of-fit tests of logistic regression analysis can employ three indicators: $-2$Log likelihood, Cox & Snell R Square, and Nagelkerke R Square. A smaller $-2$Log likelihood indicates that the Cox & Snell R Square and Nagelkerke R Square are closer to 1 and that there is a better fit of the regression model. As can be seen from Table 6, 82 samples were successfully predicted among 90 samples without water inrush, an accuracy rate of 91.1%; 31 samples were successfully predicted among 35 samples with water inrush, an accuracy rate of 88.6%. This shows that 113 samples (82 samples without water inrush and 31 samples with water inrush) had been predicted successfully from among 125 samples, with an average accuracy rate of 90.4% using logistic regression analysis of the principal components.

### Logistic Regression Analysis

Using SPSS data analysis software, logistic regression analysis was performed directly on 125 mine water inrush data points, including 90 samples without water inrush and 35 samples with water inrush (Table 7).

As shown in Table 7, 74 samples were successfully predicted among 90 samples without water inrush, an accuracy rate of 82.2%; 27 samples were successfully predicted among 35 samples with water inrush, an accuracy rate of 77.1%. This shows that 101 samples were predicted

**Table 5** The results of principal component analysis

| Principal component | Initial eigenvalues | | | The principal component score coefficients | | | | | | |
|---|---|---|---|---|---|---|---|---|---|---|
| | Characteristic root | Variance contribution rate (%) | Cumulative variance contribution rate (%) | Mining thickness | Working face slanting length | Coal seam dip angle | Mining depth | Water pressure | Cohesion | Internal friction angle |
| 1 | 2.014 | 28.776 | 28.776 | − 0.111 | − 0.375 | 0.139 | − 0.217 | 0.085 | 0.400 | 0.332 |
| 2 | 1.764 | 25.197 | 53.972 | 0.158 | 0.088 | 0.368 | − 0.290 | 0.514 | − 0.101 | − 0.201 |
| 3 | 1.337 | 19.102 | 73.075 | 0.584 | − 0.010 | 0.322 | 0.489 | − 0.023 | 0.131 | 0.216 |
| 4 | 0.875 | 12.507 | 85.582 | | | | | | | |
| 5 | 0.566 | 8.082 | 93.663 | | | | | | | |
| 6 | 0.300 | 4.291 | 97.954 | | | | | | | |
| 7 | 0.143 | 2.046 | 100.000 | | | | | | | |

successfully from 125 samples, with an average accuracy rate of only 80.8% using logistic regression analysis.

The results of the two regression analyses show that the value of − 2Log likelihood is relatively small. When the value of Cox and Snell R Square and Nagelkerke R Square was close to 1, the regression model fit better than the other models did, and the average accuracy of logistic regression analysis of the principal component was around 10% higher than that of logistic regression analysis. This is because the correlation between the main control factors of floor inrush was too strong, and the quality of the evaluation of mine water inrush was relatively poor under logistic regression analysis of the measured data. The correlations between the main control factors were greatly reduced after principal component dimension reduction, and the principal components after dimension reduction were suitable for logistic regression analysis. Therefore, the evaluation model based on logistic regression analysis of the principal component is more ideal for predicting inrush through the mine floor.

## Conclusions

Considering the potential impact of mine floor water in different directions on an inclined mining floor, a mechanical calculation model of the mining floor failure depth along the inclination direction of a coal seam was established, and the maximum failure depth of the upper and lower sides of a working face mining floor was obtained. The influence of coal seam dip angle on the floor failure depth was thoroughly considered, expanding the theoretical calculation range of floor failure depths, which provides more reference values for field measurements of mine floor failure depth.

Matrix analysis and variance analysis were used to perform a sensitivity analysis of the main control factors of floor failure depth. Using these two methods, the sensitivity of the floor failure depth factor layer is consistent with experimental results, showing that the working face slanting length is extremely significant, mining depth is highly significant, cohesion is significant, and mining thickness, dip, pressure and friction angle are not significant. Simultaneously, by utilizing matrix analysis, the optimal scheme for an orthogonal simulation test is determined, which can effectively reduce the danger of floor water inrush with the minimum floor failure depth. Thus, the matrix analysis method has more practical value than does the variance analysis method in a sensitivity analysis of the main control factors of floor failure depth.

The accuracy of the logistic regression analysis of the principal components is, on average, about 10% better than that of logistic regression analysis. The average accuracy of the floor water inrush regression model established by logistic regression analysis of the principal component is up to

**Table 6** The results of logistic regression analysis of the principal component

| Observed | | | | | | | Predicted | | |
|---|---|---|---|---|---|---|---|---|---|
| | | | | | | | Tag | | Percentage correction |
| | | | | | | | 0 | 1 | |
| Step 1 | The assessment indexes of goodness-of-fit | | | Tag | | 0 | 82 | 8 | 91.1 |
| | − 2Log likelihood | Cox & Snell R Square | Nagelkerke R Square | | | 1 | 4 | 31 | 88.6 |
| | 8.174 | 0.613 | 0.798 | Total percentage | | | | | 90.4 |

The tag 0 and 1 represent a state without water inrush and a state with water inrush, respectively

**Table 7** The results of logistic regression analysis

| Observed | | | | | | | Predicted | | |
|---|---|---|---|---|---|---|---|---|---|
| | | | | | | | Tag | | Percentage correction |
| | | | | | | | 0 | 1 | |
| Step 1 | The assessment indexes of goodness-of-fit | | | Tag | | 0 | 74 | 16 | 82.2 |
| | − 2Log likelihood | Cox & Snell R Square | Nagelkerke R Square | | | 1 | 8 | 27 | 77.1 |
| | 18.003 | 0.451 | 0.620 | Total percentage | | | | | 80.8 |

90.4%, which can quantify the actual risk of inrush through the mine floor and avoid either underestimating or overestimating the inrush risk. The recovery rate of the working face is maximally improved on the premise of ensuring safe mining. The fitting degree of the regression model is high; thus, it can be widely used for water inrush evaluation for mine floors.

# References

Cao QK, Zhao F (2011) Risk evaluation of water inrush from coal floor based on fuzzy-support vector machine. J Chin Coal Soc 36(4):633–637 **(Chinese)**

Chen K (2005) Experimental design and analysis. Tsinghua Univ Press, Beijing **(Chinese)**

Cheng JL, Yu SJ, Song Y, Cheng HL, Song ZQ (1999) Detection of the failure depth of coal seam floor by acoustic wave computer topography. J Chin Coal Soc 24(6):576–580 **(Chinese)**

Feng MM, Mao XB, Bai HB, Wang P (2009) Experimental research on fracture evolution law of water-resisting strata in coal seam floor above aquifer. Chin J Rock Mech Eng 28(2):336–341 **(Chinese)**

Gao YF, Zhang YP, Zhang HM, Wang SF (2009) Research on expert system for risk assessment of water inrush from coal floor and its application. Chin J Rock Mech Eng 28(2):253–258 **(Chinese)**

Jiang AN, Liang B (2005) Forecast of water Inrush from coal floor based on least square support vector machine. J Chin Coal Soc 30(5):613–617 **(Chinese)**

Li BY (1999) "Down Three Zones" in the prediction of water inrush from coalbed floor aquifer-theory, development and application. J Shandong I Min Tech 18(4):11–18 **(Chinese)**

Li XG, Gao YF (2003) Damage analysis of floor strata. Chin J Rock Mech Eng 22(1):35–39 **(Chinese)**

Liu WT, Liu SL, Ji BJ (2015) Sensitivity analysis of control ling factors on failure depth of floor based on orthogonal experiment. J Chin Coal Soc 40(9):1995–2001 **(Chinese)**

Lu HF, Yao DX (2014) Stress distribution and failure depths of layered rock mass of mining floor. Chin J Rock Mech Eng 33(10):2030–2039 **(Chinese)**

Peng SP, Wang JA (2001) Safe mining above confined aquifer. Coal Industry Press, Beijing **(Chinese)**

Rezaei M, Valipour M, Valipour M (2016) Modelling evapotranspiration to increase the accuracy of the estimations based on the climatic parameters. Water Conserv Sci Eng 1(3):197–207

Shi LQ, Tan XP, Wang J, Ji XK, Niu C, Xu DJ (2015) Risk assessment of water inrush based on PCA_Fuzzy_PSO_SVC. J Chin Coal Soc 40(1):167–171 **(Chinese)**

Sun J (2014) Failure characteristics of floor "three-zone" along the inclined direction of coal seam. J Min Safe Eng 1(31):115–121 **(Chinese)**

Valipour M (2016) How much meteorological information is necessary to achieve reliable accuracy for rainfall estimations? Agriculture 6(4):53. https://doi.org/10.3390/agriculture6040053

Valipour M, Banihabib ME, Behbahani SMR (2013) Comparison of the ARMA, ARIMA, and the autoregressive artificial neural network models in forecasting the monthly inflow of Dez dam reservoir. J Hydrol 476:433–441

Valipour M, Gholami Sefidkouhi MA, Raeini – Sarjaz M (2017) Selecting the best model to estimate potential evapotranspiration with respect to climate change and magnitudes of extreme events. Agr Water Manage 180(Part A): 50–60

Wang LC (2000) Method and application of mine geological radar. J Chin Coal Soc 25(1):5–9 **(Chinese)**

Wang JC, Xu YC, Xu GM, Li JB (2010) Application of mine electric profiling method to detect floor failure depth of coal mining face. Coal Sci Technol 38(1):97–100 **(Chinese)**

Wu Q, Pang W, Dai YC, Y J (2006) Vulnerability forecasting mod el based on coupling technique of GIS and ANN in floor ground water bursting. J Chin Coal Soc 31(3):314–319 **(Chinese)**

Wu Q, Wang JH, Liu DH, Cui FP, Liu SQ (2009) A new practical methodology of the coal floor water bursting evaluating IV: The application of AHP vulnerable index method based on GIS. J Chin Coal Soc 34(2):233–238 **(Chinese)**

Xu ZL (2007) Elasticity. Higher Education Press, Beijing **(Chinese)**

Zhang JC, Zhang YZ, Liu TQ (1997) Seepage of rock mass and coal floor water bursting. Geological Press, Beijing **(Chinese)**

Zhang WQ, Zhang GP, Li W, Hua X (2013) A model of Fisher's discriminant analysis for evaluating water inrush risk from coal seam floor. J Chin Coal Soc 38(10):1831–1836 **(Chinese)**

Zhou XL, Yang GY, Zheng SS (2014) Influencing factors on water burst in the roof of No. 3 seam in the Dongtan coal mine. J Min Safe Eng 1(31):115–121 **(Chinese)**